Nanoscale Diffusion of Polymer-Grafted Nanoparticles in Entangled Polymer Melts

Liquan Wang,* Jun Ma, Wei Hong, Haojing Zhang, and Jiaping Lin*

Read Online

ACCESS | Metrics & More | Article Recommendations | Supporting Information

ABSTRACT: We conducted a dissipative particle dynamics simulation on the motion of polymer-grafted nanoparticles in entangled polymer melts. Three regimes for the mean square displacement of the nanoparticles were discovered at different time scales. The nanoparticles undergo Brownian diffusion at short and long time scales and exhibit subdiffusive behavior at intermediate time scales. The short-time diffusion can be approximated as the motion of bare nanoparticles, while the long-time diffusion is associated with the entire polymer-grafted nanoparticle. The long-time Brownian diffusion was found to be non-Gaussian, which originates from the hopping diffusion of polymer-grafted nanoparticles in entangled polymer melts. The results nicely support the experimental findings and provide a comprehensive insight into the anomalous dynamics of polymer-grafted nanoparticles in polymer melts.
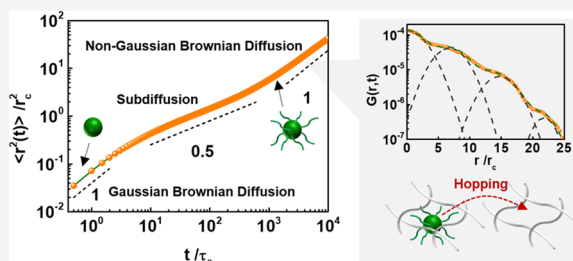
INTRODUCTION

Incorporating nanoparticles into polymeric matrices can cause a remarkable improvement in the mechanical properties of polymer nanocomposites relative to the neat polymers.[1−3] Additionally, the mobility of nanoparticles can influence the processing properties, such as the viscosity and melt flow of the polymer nanocomposites. Therefore, a deep understanding of the dynamic behavior of nanoparticles in polymer melts is of both technological and fundamental importance for optimizing both the mechanical properties and processing properties. The movement of nanoparticles in polymer melts does not always obey the Stokes−Einstein relation for Brownian diffusion, that is, the mean square displacement (MSD) is proportional to the elapsed time t ($\langle r^2 \rangle \sim t^v$ with $v = 1$) over a broad time range.[4] The nanoparticle can undergo a confined subdiffusive motion ($v < 1$) in polymer melts.[5−10] Even for Brownian diffusion, the displacement distribution in polymer melts could sometimes deviate from Gaussian forms, which is termed "anomalous yet Brownian" diffusion.[11−15]

Nanoparticles are usually functionalized by tethering polymer chains to the nanoparticle surfaces to control the dispersion of nanoparticles in polymer matrices.[16] The grafted chains tend to retard the motion of the nanoparticles, which renders the mobility of polymer-grafted nanoparticles (PGNs) much more complicated than that of bare nanoparticles.[17] Ge and Rubinstein developed a scaling theory for the motion of PGNs in unentangled polymer melts.[18] They predicted that the MSD of PGNs could be approximated by the MSD of bare nanoparticles in particle-dominated regimes and the MSD of the branch point of a star polymer in brush-dominated regimes. Despite their systematic scaling study, theoretical and simulation studies that deal with PGN mobility in entangled

polymer melts remain scarce. Entanglement, however, is a universal phenomenon in polymers due to their high molecular weight. As such, the dynamic behavior of PGNs in entangled polymer melts needs to be explored, especially for nanoparticles of a size commensurate with the correlation length of matrix polymers.

Experimentally, inconsistent conclusions have been made from different studies. Most experimental studies suggested that the diffusion of PGNs is associated with the relaxation of grafted chains and the interpenetration between grafted chains and matrix polymers.[19−21] In contrast, Winey et al. recently suggested that the grafted polymers of both moderate molecular weight and grafting density suppress nanoparticle mobility via enlarging the effective size of nanoparticles rather than through enhanced friction via entanglements between grafted chains and matrix polymers.[22] In addition, the experiments can only provide information at large length and time scales because they are limited by instrument accuracy. For example, Lungova et al. studied the mobility of polyhedral oligomeric silsesquioxane (POSS) grafted with poly(ethylene glycol) (PEG) immersed in PEG matrices using neutron spin-echo (NSE) spectrometry.[16] They observed a crossover from subdiffusion following a $t^{0.56}$ power law to Brownian diffusion in entangled matrices at the time scales longer than 1 ns, but
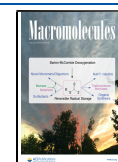
the dynamic behavior at the time scales shorter than 1 ns is unknown.

In this work, we studied the motion of PGNs in entangled polymer melts using dissipative particle dynamics (DPD) simulations. Particular attention was paid to the scaling of the MSD of nanoparticles with time and the pattern of non-Gaussian diffusion in the long-time Brownian stage. We found that the nanoparticle can undergo three-stage diffusion, that is, short-time Gaussian diffusion, intermediate-time subdiffusion, and long-time non-Gaussian diffusion, where the appearance of non-Gaussian diffusion behavior at long time scales was due to the hopping of PGNs. A comparison with existing experimental findings shows that the simulation results can support the experimental results. The present work could provide essential information for controlling nanoparticle dispersion in polymer matrices and for insight into the rheological/mechanical properties of polymer nanocomposites.

■ METHODS

We employed a mesoscopic simulation approach, that is, dissipative particle dynamics (DPD),[23−27] to investigate the motion of nanoparticles in polymer-grafted nanoparticle systems. In the DPD method, a bead represents a group of atoms. The motion of the beads obeys Newton's equation of motion $d\mathbf{r}_i/dt = \mathbf{v}_i$ and $md\mathbf{v}_i/dt = \mathbf{f}_i$, where $\mathbf{r}_i$, $\mathbf{v}_i$, $\mathbf{f}_i$, and m_i are the position, velocity, total force, and mass of ith bead, respectively. For an unentangled polymer, four pairwise forces are usually applied to describe the interaction between ith and jth beads, that is, a conservative force $\mathbf{F}_{ij}^C$, a dissipative force $\mathbf{F}_{ij}^D$, a random force $\mathbf{F}_{ij}^R$, and a spring bond force $\mathbf{F}_{ij}^S$. The interaction force between the two bonded beads of each matrix copolymer (or graft chain) is given as a harmonic spring force $\mathbf{F}_{ij}^S = C(1 - r_{ij}/r_{eq})\hat{\mathbf{r}}_{ij}$ with a spring constant $C = 100$ and an equilibrium bond distance $r_{eq} = 0.86$ r_c (r_c is a cutoff distance). For an entangled polymer, the modified segmental repulsive potential (mSRP),[28] developed by Sirk et al. based on the work of Kumar and Larson,[29,30] was also applied to remove unphysical chain crossings in DPD simulations. The mSRP is given as

$$\mathbf{F}_{kl}^{mSRP} = B(1 - d_{kl}/d_c)\hat{\mathbf{d}}_{kl} \qquad (1)$$

where B is a force constant, d_c is the bond−bond cutoff distance, and d_{kl} and $\hat{\mathbf{d}}_{kl}$ are the midpoint-to-midpoint distance and the unit vector between kth and lth bonds, respectively. For the ith and jth beads in the kth bond, this force is decomposed into bead forces: $\mathbf{F}_i = \mathbf{F}_{kl}^{mSRP}/2$ and $\mathbf{F}_j = \mathbf{F}_{kl}^{mSRP}/2$. Segmental repulsion interactions for adjacent bonds were excluded. We adopted the parameters recommended by Sirk et al., that is, $B = 100$, $d_c = 0.8$, and $k_\theta = 2.0$.[28] Here, k_θ is a force constant for the angle bending potential $U_{bend} = k_\theta(1 + \cos\theta)$ (θ is the angle formed by two consecutive bonds). For the details of the DPD method, see Section 1 of the Supporting Information.

The PGN consists of eight polymer chains with one end uniformly grafted to the surface of a spherical nanoparticle (see Figure 1). The spherical nanoparticle was treated as a dodecahedron consisting of 20 vertex beads and a center bead. The harmonic spring force with $C = 300$ and $r_{eq} = 0.5r_c$ was applied to two closet vertex beads. The harmonic spring force with $C = 300$ and $r_{eq} = 0.7r_c$ was applied between the center bead and the vertex bead. The radius R_b of the nanoparticle is ca. 1.5 times the equilibrium center-to-vertex distance, that is, $R_b = 1.05r_c$. An angle potential in the form of $\mathbf{F}^A = -k(\theta - \theta_0)$ is applied to two closed bonds on the surface of the dodecahedron, where $k = 300$ and $\theta_0 = 108°$ in this work. Such treatment is to ensure that the nanoparticles are a rigid body. The interaction strengths between all species are 25, and therefore, the system is athermal.

All the simulations were performed using the Large-scale Atomic/Molecular Massively Parallel Simulator (LAMMPS) software.[31] In the simulation, the standard DPD was first carried out to equilibrate the polymer structures ($t = 1000\tau$), and then the mSRP was turned on. The time step of $\Delta t = 0.005\tau_0$ was chosen to ensure the numerical
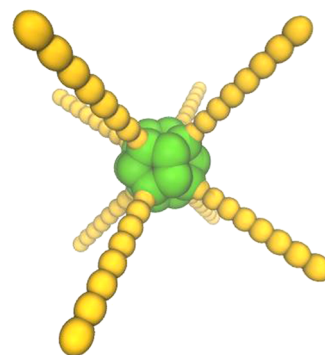

Figure 1. Coarse-grained model of polymer-grafted nanoparticles, where the nanoparticle and grafted chains are colored in green and yellow, respectively.

stability of the simulation and smaller topology violations.[28] The time unit τ_0 can be formulated by $\tau_0 = \sqrt{mr_c^2/k_B T}$, where m, r_c, τ_0, and $k_B T$ are the units of mass, length, time, and energy, respectively.

■ RESULTS AND DISCUSSION

We considered several PGNs diffusing in a linear polymer melt. The PGN consists of eight polymer chains with one end uniformly grafted to the surface of a spherical nanoparticle with radius $R_b \sim 1.05r_c$ (see Figure 1 and the inset of Figure 2a),
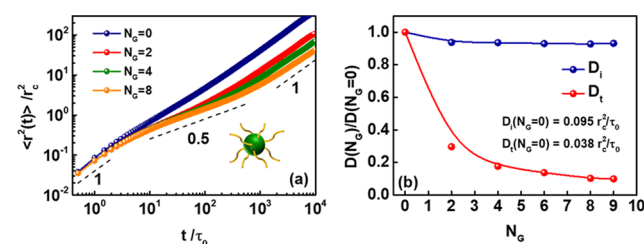

Figure 2. (a) Time dependence of the mean square displacement $\langle r^2 \rangle$ of nanoparticles, where the length N_P of the matrix polymers is 40. The inset shows the model of polymer-grafted nanoparticles. (b) Plots of the initial and terminal diffusion coefficients D scaled by the diffusion coefficients for bare nanoparticles as a function of the length N_G of grafted chains.

which could be the prototype model of representative POSS grafted with PEG.[16] The concentration of PGNs is so dilute that the PGNs move individually in polymer melts. We assumed that the grafted polymers with N_G monomers per chain and the matrix polymers with N_P monomers per chain in the melt are chemically identical, and therefore, the PGNs in the polymer matrix can be considered nonsticky athermal nanoparticles without enthalpic interaction.[16] The segmental repulsive potential was introduced into the DPD simulation to simulate the entanglement effect in polymer melts.[28−30] In the polymer melt, whether or not the polymers (or grafted chains) are entangled depends upon the length of the polymers (note that the entanglement length is $N_P = 14$ and the tube diameter a is ca. $4r_c$).[28]

The mobility of PGNs in the polymer melt was quantified by the time dependence of their MSD. Figure 2a shows the representative results of the calculated MSDs. In this simulation, the matrix polymers were chosen to be long enough ($N_P = 40$) to guarantee that the polymers in melts are interentangled. One can see that the MSD behaviors vary from a short-time linear stage to a sublinear stage and to a long-time

linear stage. The slopes v of the MSDs in logarithmic coordinates for the three stages are very close to 1.0, 0.5, and 1.0, which are consistent with those for nonsticky nanoparticles of intermediate size ($\xi < d < a$; ξ: correlation length; d: particle diameter) in entangled polymer melts.[32] According to the slopes, three regimes can be distinguished, that is, initial Brownian diffusion, subdiffusion, and terminal Brownian diffusion. Moreover, the MSD curves shift downward with increasing the length N_G of grafted chains, implying that the mobility of the nanoparticles is reduced as the grafted chains become longer because the grafted polymers tend to suppress the motion of nanoparticles.

Notably, the MSD curves in a short time almost overlap, which indicates the independence of short-time diffusion on the grafted polymers. This behavior can be clearly illustrated by examining the diffusion coefficients D that quantify the motion of nanoparticles. Figure 2b presents the diffusion coefficients for short-time diffusion and long-time diffusion. As shown, the D_i for short-time diffusion is nearly unchanged with the length of the grafted chains, which means that the MSD of PGNs at a short time can be approximated by that of bare nanoparticles. At short time scales, the motion of the nanoparticle center is diffusive, as they "feel" the local viscosity comparable to that of monomers; the grafted chains and polymers behave the same because the time scale is smaller than the relaxation time of a correlation blob with size ξ ($\approx 0.7r_c$, i.e., the average distance from a bead to the nearest bead). As the time scale increases, the hydrodynamic diameter of the nanoparticles increases, and the D_t for terminal diffusion decreases with increasing the length of grafted chains. The hydrodynamic radius R can then be evaluated according to the scaling law $D_t \sim R^{-3}$.[32] For example, the R for $N_G = 6$ is approximately 2 times the radius R_b of bare nanoparticles (see Figure S1), and therefore, the hydrodynamic diameter $2R$ of the PGNs is comparable to the tube diameter a ($\sim 4r_c$). The scaling law $R \sim N_G^{1/4}$ suggests that the grafted chains retard the mobility of the nanoparticle by enlarging the effective size of the nanoparticles, which supports the observation of Winey et al.[22]

The self-intermediate scattering function, $F(\mathbf{q}, t) = \frac{1}{N} \left\langle \sum_{j=0}^{N} \exp[i\mathbf{q}(\mathbf{r}_j(t) - \mathbf{r}_j(0))] \right\rangle$, was calculated to measure the dynamics of the nanoparticles. $F(\mathbf{q},t)$ is plotted in Figure S2 as a function of time for a series of wave vectors $\mathbf{q}$. The observed dynamics slow considerably with decreasing q. We found that the decrease in $F(\mathbf{q},t)$ with time is slower than the exponential decay in time by fitting the curves in Figure S2 with a stretched exponential $\exp[-(t/\tau_r(q))^{\beta(q)}]$. The plots of the relaxation time τ_r and the stretched exponent β as a function of q are given in Figure 3a,b, respectively. At small q, τ_r scales with q^{-2} and β approaches one, which implies that the
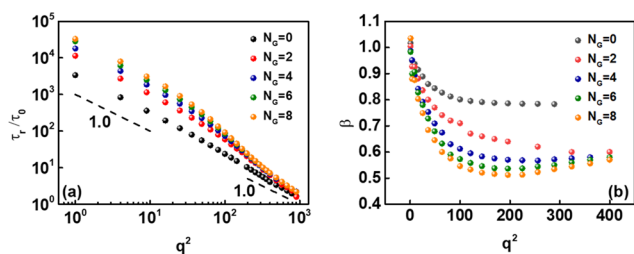
nanoparticles exhibit Brownian diffusion at large length and time scales. With increasing q value, τ_r decreases and β first decreases and then increases. At large q, the τ_r values that scale with q^{-2} are almost the same for various numbers N_G of grafted chains, which is consistent with the observation of MSD at short time scales (see Figure 2a). For fixed q, τ_r increases, and β decreases as the number N_G of grafted chains increases.

In addition to the length of grafted chains, the grafting density could impact the motion of PGNs. Recently, Rubinstein et al. have established the relation between the effective size of the PGN with grafting density.[18] The relation depends on the relative magnitudes of the grafting density (the number z of grafted chain per PGN), the length N_G of grafted chains, and the length N_P of matrix polymers. For most cases, the radius R of PGNs scales positively with the number z of grafted chains, that is, $R \sim z^{1/3}$ or $R \sim z^{1/5}$. Only as $z^2 < N_G < (N_P/z)^2$, the radius of PGNs is independent of the number of grafted chains. As such, the increase in grafting density could enlarge the effective size of the PGN. Because the effective viscosity "felt" by the particles at long times is proportional to the number of correlation blobs in a chain section with a size comparable to nanoparticle diameter,[32] the slowdown of the nanoparticle motion could be expected as the grafting density of PGNs increases.

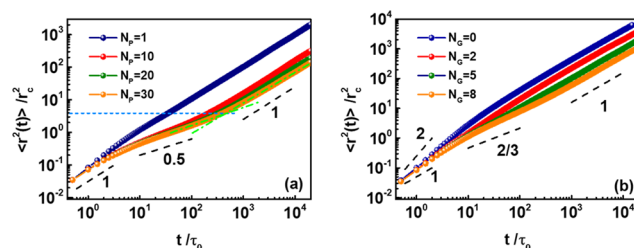The effect of the length N_P of the matrix polymers on the MSD was also investigated. The result is shown in Figure 4a,

Figure 4. (a) Time dependence of the mean square displacement $\langle r^2 \rangle$ for the PGN systems with various lengths N_P of the matrix polymer, where the length N_G of the grafted chain on the nanoparticles is 5. The horizontal short dashed line (light blue) indicates the MSD values that separate the subdiffusive regimes from the long-time diffusion regime. (b) Time dependence of the mean square displacement $\langle r^2 \rangle$ for the PGN solutions with various lengths N_G of the grafted chain, where the length N_P of the matrix polymer is 1.

Figure 3. Plots of the (a) relaxation time τ_r and (b) stretched exponent β as a function of wave vectors q^2.

where the $\langle r^2 \rangle$ for PGNs with $N_G = 5$ is plotted as a function of the time interval. For the PGNs in the athermal solvents ($N_P = 1$), the MSD behavior changes from a short-time diffusion stage to a long-time diffusion stage, and subdiffusion with $v \approx 2/3$ appears at the intermediate time scale due to the Zimm dynamics of PGNs.[18] Such a behavior holds for PGNs with varied lengths N_G of grafted chains (see Figure 4b). As N_P is higher than 10, the MSD curves tend to overlap not only at the short-time stage but also at the long-time stage. The matrix polymers tend to be entangled under this condition, and therefore, the motion of nanoparticles is only dependent upon the entanglement length but is independent of the length of matrix polymers. As demonstrated by Sirk et al., the entanglement length is 14 in this DPD simulation,[28] close to the value of N_P that appears to have a less marked effect on the MSD behaviors. The crossover from subdiffusion to long-time diffusion occurs at $\langle r^2 \rangle \approx 4r_c^2$, which matches the square hydrodynamic radius of a PGN.

The MSD only holds information for second-order moments, and therefore, non-Gaussian parameters, $\alpha_2(t) = 3\langle\Delta r^4(t)\rangle/5\langle\Delta r^2(t)\rangle^2 - 1$, containing fourth-order moments, are evaluated to gain more information regarding the diffusion of PGNs.[11,33] Generally, $\alpha_2 = 0$ indicates a Gaussian diffusion behavior. Figure 5 shows the variation in non-Gaussian
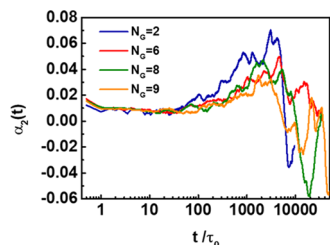

Figure 5. Non-Gaussian parameters $\alpha_2(t)$ as a function of elapsed times for the PNGs with various lengths N_G of grafted chains, where the length N_P of the matrix polymer is 40.

parameters as a function of the time interval. The $\alpha_2(t)$ function approaches zero at a short time scale, implying the Gaussian diffusion of nanoparticle centers. As the time interval increases, $\alpha_2(t)$ deviates from the zero value, which implies that the diffusion of nanoparticle centers becomes non-Gaussian. Note that $\alpha_2(t)$ at long time scales fluctuates, which could be associated with the hopping diffusion of nanoparticles.

One can see from above that the anomalous yet Brownian diffusion behavior exists as the elapsed time is higher than ca. $1000\tau_0$, that is, the MSD remains linear with time, yet the non-Gaussian parameter $\alpha_2(t)$ deviates from Gaussian forms. To shed light upon the microscopic origin of this behavior, we analyzed the displacement probability distribution (DisPD) in the long-time regime. The DisPD, representing the density probability of finding a nanoparticle at a distance r from the initial position after a time interval t, can be obtained by multiplying the self-part of the von Hove function, $G(r,t) = \langle\delta(\mathbf{r} - |\mathbf{r}_i(t) - \mathbf{r}_i(0)|)\rangle$, by a factor of $4\pi r^2$. Logarithmic plots of $G(r,t)$ against the displacement normalized by the cutoff distance r_c are shown in Figure 6a. As shown, $G(r,t)$ tends to
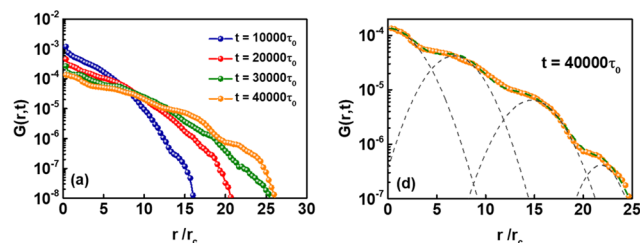

Figure 6. (a) Displacement distribution function for PGNs with $N_G = 9$. (b) The decomposition of displacement distributions into four Gaussian distributions (gray dashed lines) at the time intervals of $t = 40\,000\tau_0$.

deviate from the unimodal Gaussian distribution. Instead, multimodal distributions are observed, in particular, on a long time scale. The $G(r,t)$ curves can be decomposed into several unimodal Gaussian distributions with different peak positions (see the dashed lines in Figure 6b). For example, $G(r,t)$ consists of four Gaussian distributions at $t = 40\,000\tau_0$ (Figure

6b). The DisPD shows the apparent derivation from the Gaussian distribution at long time scales (see Figure S3).

The existence of multiple unimodal Gaussian distributions in each $G(r,t)$ curve implies that there are similar distributions after every time interval, corresponding to the Gaussian diffusion of nanoparticles in different local regions. The time intervals between different distributions are associated with the hopping effect of PGNs in the entangled polymer melts. To see such a hopping phenomenon, we recorded the representative trajectory of a PGN, which is shown in Figure 7. The particles
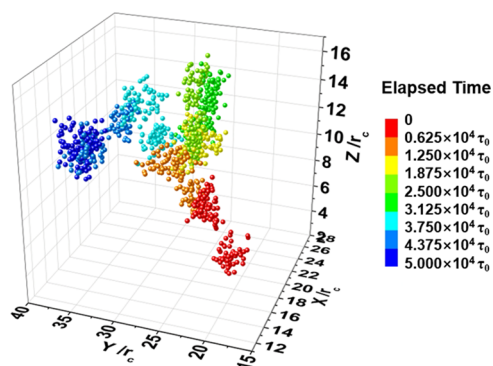

Figure 7. Typical motion trajectory of the nanoparticle center of a PGN with $N_G = 8$. Different colors are assigned to different elapsed times.

spend most of the time in diffusing in a local confined region and sometimes escape from this confined region as a rare event. This escaping behavior is usually referred to as the hopping effect. In the present system, the separation of time scales—the diffusion of nanoparticles and the relaxation of the polymers (see Figures 3a and S5)—is not so large that the anomalous yet Brownian diffusion behavior was observed.[12] The slow environment changes (polymer relaxation) in space and time cause the derivation of the DisPD from the Gaussian distribution.

We found that the bare nanoparticles with $R_b \sim 1.05r_c$ can even hop in the polymer melt with $a \sim 4r_c$ (see Figure S4). This is in contrast to the theoretical prediction that hopping is relevant only for nanoparticles with $2R/a \sim 1.5-2$.[34,35] Recently, Lyulin et al. also found that hopping can take place for the system with very small $2R/a$ ($\sim$0.1).[36] However, they suggested that the attraction between polymers and nanoparticles contributes much to the hopping effect for small nanoparticles. Kalathi et al. also suggested that the hopping mechanism may play an essential role in the nanoparticle motion for nanoparticles comparable to the entanglement length as the nanoparticle−polymer interaction becomes attractive.[37]

In contrast, in our system, the polymer and nanoparticles are athermal relative to each other, and the polymers are slightly entangled. As such, an important question arises as to whether the polymer−nanoparticle attraction is necessary for the hop-like motion of nanoparticles comparable to the entanglement length or not. Very recently, Composto et al. found that the nanoparticles are localized within two regions, that is, a narrow primary localized region due to the nanoparticle−polymer attraction and a broad secondary localization region due to network confinement.[38] Their work implies that in addition to the attraction between nanoparticles and polymers, the network confinement plays a vital role in determining the

hopping mechanism of nanoparticles with a size much smaller than the network mesh size. Note that the nanoparticles are quantum dots with a hydrodynamic diameter of 10 nm, and the secondary localization regions are in the size of 150−200 nm. This result could support the existence of hop-like motion in our system.

To gain insight into the effect of N_G on the hopping mechanism, we calculated the displacement correlation (DC) function that qualifies the time correlation between the consecutive displacements of time interval t. The DC function is given as $\mathrm{DC}(t) = \langle \delta \mathbf{r}(t_0,t)\delta \mathbf{r}(t_0 - t,t)\rangle$, where $\delta \mathbf{r}(t_0,t) = \mathbf{r}(t_0 + t) - \mathbf{r}(t)$.[36,39] Figure 8 shows the log–log plots of the
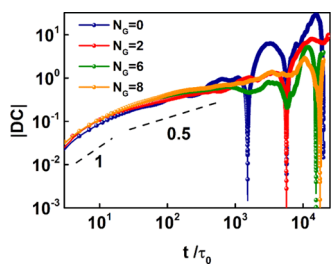

Figure 8. Log−log plots of the absolute values of DC functions as a function of the time interval for PGNs with various values of N_G.

absolute values of DC functions as a function of the time interval for PGNs with various values of N_G. In a short time interval, the slope of the curve is ca. 1, yielding the Hurst exponent H of 0.5 (note that $\mathrm{DC}(t) \sim t^{2H}$). This indicates a tendency for the displacement to be uncorrelated in normal Brownian motion. On intermediate time scales, H is ca. 0.25, implying that the DC is anticorrelated in the subdiffusive regime. Beyond this time, the "peak" appears, which may refer to the typical time when the hopping occurs. As shown, the first apparent peak shift to high values of time intervals as N_G increases. This implies that more "waiting" time is required for PGNs with larger N_G to escape from polymer cages.

The dynamics of PGNs in polymer melts have been studied experimentally.[19−22,40] Various characterization techniques such as X-ray photon correlation spectroscopy (XPCS), Rutherford backscattering spectrometry (RBS), and neutron spin-echo spectrometry (NSE) were employed in the experiments. Generally, experimental measurements can only provide information at large length and time scales due to the limitation of instrument accuracy. Our simulation, however, is able to provide information spanning a broader range of time and space scales, which can not only compare with existing experiment findings but also supplement to the experiments.

Lungova et al. studied the motion of POSS grafted with PEG immersed in PEG matrices by NSE.[16] They found that the MSD of POSS in entangled PEG crosses over from subdiffusion following a $t^{0.56}$ power law to Brownian diffusion at a long time scale. This finding is similar to our observation shown in Figure 2a, since the exponent of 0.56 is very close to the theoretical value of 0.5. Guo et al. investigated the motion of gold nanoparticles in low-molecular-weight polystyrene (PS) melt using XPCS, where the gold surface is functionalized with thiol-terminated PS chains.[41] Their results showed that at high temperatures (323 and 333 K, where T_g is 292 K), the relaxation time τ_r decreases with the wave vector q as $\tau_r \sim q^{-2}$ when q is small. As q increases, the exponent derivates from −2. (Note that Guo et al. did not point out this derivation, but

such a derivation does exist, as shown in Figure 3 of their work.) Such a variation is consistent with our finding that the τ_r scales with q^{-2} at smaller q and a derivation appears as q increases (see Figure 3a). This experimental finding may correspond to the simulation cases where q is not very large because the scaling relation $\tau_r \sim q^{-2}$ can recover at large q. Lungova et al. also observed subdiffusion with the scaling relation $\langle r^2 \rangle \sim t^{0.77}$ in an untangled melt.[16] The exponent of 0.77 is close to the exponent of 0.8 in the scaling law for the subdiffusion of nanoparticles in polymers with $N_P = 1$ (see Figure 4b). We suggest that such a scaling law results from the coupling between the motion of PGNs and the Zimm dynamics of the surrounding solvents.

Winey et al. used RBS to measure the diffusion of poly(methyl methacrylate) (PMMA)-grafted nanoparticles in unentangled or slightly entangled PMMA melts.[22] They found that the diffusion coefficient of nanoparticles decreases as the molecular weight of matrix polymers increases. We also observed similar phenomena as the matrix polymers are not very long, that is, the nanoparticles move slowly as the length of the matrix polymers increases (see Figure 4a). However, we found that the MSD of nanoparticles becomes indistinguishable for longer matrix polymers, suggesting that the diffusion of nanoparticles is almost independent of the matrix polymer length as the polymer length exceeds the entanglement length. Because Winey's work only centers on unentangled and slightly entangled melts (probably corresponding to the simulation case where N_P is smaller than 20), the independence of the MSD on the molecular weight of the matrix polymers was not shown.

In a very recent study, Winey et al. measured the diffusion of octa(aminophenyl) polyhedral oligomeric silsesquioxane (OAPS) nanoparticles in well-entangled poly(2-vinylpyridine) (P2VP).[42] They found that the OAPS diffusion coefficients scale very weak with the molecular weight of P2VP. Their results suggest that the weak molecular weight dependence is coupled with polymer dynamics between segment relaxations and Rouse relaxations due to the weak attraction between OAPS and P2VP. Since our system is athermal, the independence of diffusion coefficients on molecular weight could be expected in our simulation, and we did find that the MSD becomes indistinguishable as the polymer is longer (see Figure 4a). This is because, in our systems, the nanoparticle motion is coupled with the relaxation of polymer segments (approximately molecular weight independence).

Composto et al. measured the nanoparticle diffusion in gels by single-particle tracking.[38,43] They found that the diffusion of nanoparticles depends on the mesh sizes that can be tuned by varying crosslinker density, adding poor solvents, or changing temperatures. The mobile nanoparticles displayed either intermittent localization or continual diffusion. The intermittent localization corresponds to the hopping effect in our simulation, as the nanoparticle escapes from the mesh network to be localized elsewhere. In addition, they found that van Hove distributions exhibit non-Gaussian displacements and can be fit by double Gaussians.[38] Such a finding is consistent with our results shown in Figure 6b. Of particular interest is that they observed a combination of intermittent localization and continual diffusion in the gels due to network heterogeneity. However, such a phenomenon was not observed in our systems, probably due to the relatively uniform entangled network (not crosslinked as in their experiment).

The present work shows that the DPD simulation with modified segmental repulsive potentials can capture the hopping effect that is unlikely to obtain in the simulation based on the bead-spring model.[36,37] The hopping effect, which does not occur in unentangled polymers, is a representative phenomenon in entangled polymer melts. We found that the scaling law for nonsticky bare nanoparticles in entangled polymers can essentially apply to the present PGN system.[32] However, the mobility of PGNs in entangled polymer melts is dominated by the bare nanoparticle and the entire PGN at different time scales, as in unentangled polymer melts.[18] The deep understanding of the mobility of PGNs in polymer melts can help improve the currently available processing techniques to optimize the properties of advanced nanocomposite materials.

CONCLUSIONS

We studied the dynamic behavior of PGNs in entangled polymer melts through the DPD simulation coupled with a modified segment repulsive potential. The results show that the nanoparticle undergoes three-stage diffusion behavior, including short-time Gaussian diffusion, intermediate-time subdiffusion, and long-time non-Gaussian diffusion. The hopping of nanoparticles in the polymer melts contributes to long-time non-Gaussian diffusion. The results support the experimental findings that the grafted polymer chains retard the motion of the nanoparticle by enlarging its effective size. We expect that this work could provide valuable information for controlling nanoparticle dispersion in polymers and for understanding the rheological or mechanical properties of polymer nanocomposites.

ASSOCIATED CONTENT

Ⓢ Supporting Information

The Supporting Information is available free of charge at https://pubs.acs.org/doi/10.1021/acs.macromol.0c00721.

Simulation method and model; radius of polymer-grafted nanoparticles; self-intermediate scattering function; displacement distribution function; and relaxation of the polymers in polymer melts (PDF)

AUTHOR INFORMATION

Corresponding Authors

Liquan Wang — Shanghai Key Laboratory of Advanced Polymeric Materials, Key Laboratory for Ultrafine Materials of Ministry of Education, School of Materials Science and Engineering, East China University of Science and Technology, Shanghai 200237, China; ⊙ orcid.org/0000-0002-5141-8584; Email: lq_wang@ecust.edu.cn

Jiaping Lin — Shanghai Key Laboratory of Advanced Polymeric Materials, Key Laboratory for Ultrafine Materials of Ministry of Education, School of Materials Science and Engineering, East China University of Science and Technology, Shanghai 200237, China; ⊙ orcid.org/0000-0001-9633-4483; Email: jlin@ecust.edu.cn

Authors

Jun Ma — Shanghai Key Laboratory of Advanced Polymeric Materials, Key Laboratory for Ultrafine Materials of Ministry of Education, School of Materials Science and Engineering, East China University of Science and Technology, Shanghai 200237, China

Wei Hong — Shanghai Key Laboratory of Advanced Polymeric Materials, Key Laboratory for Ultrafine Materials of Ministry of Education, School of Materials Science and Engineering, East China University of Science and Technology, Shanghai 200237, China

Haojing Zhang — Shanghai Key Laboratory of Advanced Polymeric Materials, Key Laboratory for Ultrafine Materials of Ministry of Education, School of Materials Science and Engineering, East China University of Science and Technology, Shanghai 200237, China

Complete contact information is available at:
https://pubs.acs.org/10.1021/acs.macromol.0c00721

Notes

The authors declare no competing financial interest.

REFERENCES

(1) Balazs, A. C.; Emrick, T.; Russell, T. P. Nanoparticle polymer composites: Where two small worlds meet. Science 2006, 314, 1107−1110.

(2) Karatrantos, A.; Composto, R. J.; Winey, K. I.; Clarke, N. Polymer and spherical nanoparticle diffusion in nanocomposites. J. Chem. Phys. 2017, 146, No. 203331.

(3) Kumar, S. K.; Benicewicz, B. C.; Vaia, R. A.; Winey, K. I. 50th anniversary perspective: Are polymer nanocomposites practical for applications? Macromolecules 2017, 50, 714−731.

(4) Einstein, A. Über die von der molekularkinetischen Theorie der Wärme geforderte Bewegung von in ruhenden Flüssigkeiten suspendierten Teilchen. Ann. Phys. 1905, 322, 549−560.

(5) Tolić-Nørrelykke, I. M.; Munteanu, E.-L.; Thon, G.; Oddershede, L.; Berg-Sørensen, K. Anomalous diffusion in living yeast cells. Phys. Rev. Lett. 2004, 93, No. 078102.

(6) Weber, S. C.; Spakowitz, A. J.; Theriot, J. A. Bacterial chromosomal loci move subdiffusively through a viscoelastic cytoplasm. Phys. Rev. Lett. 2010, 104, No. 238102.

(7) Chubynsky, M. V.; Slater, G. W. Diffusing diffusivity: A model for anomalous, yet Brownian, diffusion. Phys. Rev. Lett. 2014, 113, No. 098302.

(8) Tuteja, A.; Mackay, M. E.; Narayanan, S.; Asokan, S.; Wong, M. S. Breakdown of the continuum Stokes−Einstein relation for nanoparticle diffusion. Nano Lett. 2007, 7, 1276−1281.

(9) Maldonado-Camargo, L.; Rinaldi, C. Breakdown of the Stokes−Einstein relation for the rotational diffusivity of polymer grafted nanoparticles in polymer melts. Nano Lett. 2016, 16, 6767−6773.

(10) Dai, L.; Fu, C.; Zhu, Y.; Sun, Z. Heterogeneous dynamics of unentangled chains in polymer nanocomposites. J. Chem. Phys. 2019, 150, No. 184903.

(11) Wang, B.; Anthony, S. M.; Bae, S. C.; Granick, S. Anomalous yet Brownian. Proc. Natl Acad. Sci. U.S.A. 2009, 106, 15160−15164.

(12) Wang, B.; Kuo, J.; Bae, S. C.; Granick, S. When Brownian diffusion is not Gaussian. Nat. Mater. 2012, 11, 481−485.

(13) Chen, T.; Qian, H.; Lu, Z. Diffusion dynamics of nanoparticle and its coupling with polymers in polymer nanocomposites. Chem. Phys. Lett. 2017, 687, 96−100.

(14) Phillies, G. D. J. Is complex fluids the Gaussian diffusion approximation is generally valid. Soft Matter 2015, 11, 580−586.

(15) Xue, C.; Zheng, X.; Chen, K.; Tian, Y.; Hu, G. Probing non-Gaussianity in confined diffusion of nanoparticles. J. Phys. Chem. Lett. 2016, 7, 514−519.

(16) Lungova, M.; Krutyeva, M.; Pyckhout-Hintzen, W.; Wischnewski, A.; Monkenbusch, M.; Allgaier, J.; Ohl, M.; Sharp,

M.; Richter, D. Nanoscale motion of soft nanoparticles in unentangled and entangled polymer matrices. *Phys. Rev. Lett.* **2016**, *117*, No. 147803.

(17) Medidhi, K. R.; Padmanabhan, V. Diffusion of polymer-grafted nanoparticles in a homopolymer matrix. *J. Chem. Phys.* **2019**, *150*, No. 044905.

(18) Ge, T.; Rubinstein, M. Mobility of polymer-tethered nanoparticles in unentangled polymer melts. *Macromolecules* **2019**, *52*, 1536−1545.

(19) Hoshino, T.; Murakami, D.; Tanaka, Y.; Takata, M.; Jinnai, H.; Takahara, A. Dynamical crossover between hyperdiffusion and subdiffusion of polymer-grafted nanoparticles in a polymer matrix. *Phys. Rev. E* **2013**, *88*, No. 032602.

(20) Kandar, A. K.; Srivastava, S.; Basu, J. K.; Mukhopadhyay, M. K.; Seifert, S.; Narayanan, S. Unusual dynamical arrest in polymer grafted nanoparticles. *J. Chem. Phys.* **2009**, *130*, No. 121102.

(21) Liu, S.; Senses, E.; Jiao, Y.; Narayanan, S.; Akcora, P. Structure and entanglement factors on dynamics of polymer-grafted nanoparticles. *ACS Macro Lett.* **2016**, *5*, 569−573.

(22) Lin, C.; Griffin, P. J.; Chao, H.; Hore, M. J. A.; Ohno, K.; Clarke, N.; Riggleman, R. A.; Winey, K. I.; Composto, R. J. Grafted polymer chains suppress nanoparticle diffusion in athermal polymer melts. *J. Chem. Phys.* **2017**, *146*, No. 203332.

(23) Hoogerbrugge, P. J.; Koelman, J. M. V. A. Simulating microscopic hydrodynamic phenomena with dissipative particle dynamics. *Europhys. Lett.* **1992**, *19*, 155−160.

(24) Koelman, J. M. V. A.; Hoogerbrugge, P. J. Dynamic simulations of hard-sphere suspensions under steady shear. *Europhys. Lett.* **1993**, *21*, 363−368.

(25) Groot, R. D.; Warren, P. B. Dissipative particle dynamics: Bridging the gap between atomistic and mesoscopic simulation. *J. Chem. Phys.* **1997**, *107*, 4423−4435.

(26) Li, Q.; Wang, L.; Lin, J.; Zhang, L. Distinctive phase separation dynamics of polymer blends: Roles of Janus nanoparticles. *Phys. Chem. Chem. Phys.* **2019**, *21*, 2651−2658.

(27) Lv, Y.; Wang, L.; Wu, F.; Gong, S.; Wei, J.; Lin, S. Self-assembly and stimuli-responsive behaviours of side-chain liquid crystalline copolymers: a dissipative particle dynamics simulation approach. *Phys. Chem. Chem. Phys.* **2019**, *21*, 7645−7653.

(28) Sirk, T.; Sliozberg, Y.; Brennan, J.; Lisal, M.; Andzelm, J. An enhanced entangled polymer model for dissipative particle dynamics. *J. Chem. Phys.* **2012**, *136*, No. 134903.

(29) Kumar, S.; Larson, R. G. Brownian dynamics simulations of flexible polymers with spring-spring repulsions. *J. Chem. Phys.* **2001**, *114*, 6937−6941.

(30) Pan, G.; Manke, C. W. Developments toward simulation of entangled polymer melts by dissipative particle dynamics (DPD). *Int. J. Mod. Phys. B* **2003**, *17*, 231−235.

(31) LAMMPS Molecular Dynamics Simulator. https://lammps.sandia.gov/ (accessed July 7, 2020).

(32) Cai, L.; Panyukov, S.; Rubinstein, M. Mobility of nonsticky nanoparticles in polymer liquids. *Macromolecules* **2011**, *44*, 7853−7863.

(33) Rahman, A. Correlations in the motion of atoms in liquid argon. *Phys. Rev.* **1964**, *136*, No. A405.

(34) Dell, Z. E.; Schweizer, K. S. Theory of localization and activated hopping of nanoparticles in crosslinked networks and entangled polymer melts. *Macromolecules* **2014**, *47*, 405−414.

(35) Cai, L.; Panyukov, S.; Rubinstein, M. Hopping diffusion of nanoparticles in polymer matrices. *Macromolecules* **2015**, *48*, 847−862.

(36) Volgin, I. V.; Larin, S. V.; Abad, E.; Lyulin, S. V. Molecular dynamics simulations of fullerene diffusion in polymer melts. *Macromolecules* **2017**, *50*, 2207−2218.

(37) Kalathi, J. T.; Yamamoto, U.; Schweizer, K. S.; Grest, G. S.; Kumar, S. K. Nanoparticle diffusion in polymer nanocomposites. *Phys. Rev. Lett.* **2014**, *112*, No. 108301.

(38) Parrish, E.; Seeger, S. C.; Composto, R. J. Temperature-dependent nanoparticle dynamics in poly(N-isopropylacrylamide) gels. *Macromolecules* **2018**, *51*, 3597−3607.

(39) Jeon, J.-H.; Metzler, R. Fractional Brownian motion and motion governed by the fractional Langevin equation in confined geometries. *Phys. Rev. E* **2010**, *81*, No. 021103.

(40) Choi, J.; Hore, M. J. A.; Clarke, N.; Winey, K. I.; Composto, R. J. Nanoparticle brush architecture controls polymer diffusion in nanocomposites. *Macromolecules* **2014**, *47*, 2404−2410.

(41) Guo, H.; Bourret, G.; Corbierre, M. K.; Rucareanu, S.; Lennox, R. B.; Laaziri, K.; Piche, L.; Sutton, M.; Harden, J. L.; Leheny, R. L. Nanoparticle motion within glassy polymer melts. *Phys. Rev. Lett.* **2009**, *102*, No. 075702.

(42) Bailey, E. J.; Griffin, P. J.; Composto, R. J.; Winey, K. I. Multiscale dynamics of small, attractive nanoparticles and entangled polymers in polymer nanocomposites. *Macromolecules* **2019**, *52*, 2181−2188.

(43) Parrish, E.; Caporizzo, M. A.; Composto, R. J. Network confinement and heterogeneity slows nanoparticle diffusion in polymer gels. *J. Chem. Phys.* **2017**, *146*, No. 203318.